Progress In Electromagnetics Research, PIER 81, 135–148, 2008

HIGH-FREQUENCY EXPRESSION FOR THE FIELD IN THE CAUSTIC REGION OF A PEMC GREGORIAN SYSTEM USING MASLOV'S METHOD

M. A. Fiaz, A. Aziz, A. Ghaffar, and Q. A. Naqvi

Electronics Department
Quaid-i-Azam University
Islamabad, Pakistan

Abstract—Method proposed by Maslov has been used, to remedy the problem of geometrical optics, for a two dimensional Perfect electromagnetic conductor (PEMC) Gregorian system. It generates an integral form of solution near the caustic that can be evaluated analytically/numerically, or with uniform asymptotic techniques. Away from the caustic it recovers the geometrical optics field. Numerical computations are made to calculate the field around the caustic of a Gregorian system.

1. INTRODUCTION

Perfect electromagnetic conductor (PEMC) is a non-reciprocal generalization of both perfect electric conductor (PEC) and perfect magnetic conductor (PMC). Possibilities for the realization of a PEMC boundary has been suggested by Lindell [1, 2] in terms of a layer of certain non reciprocal materials resting on a PEC plane. Parameters of a bi-isotropic medium can be chosen so that the interface of the layer acts as a PEMC boundary. The boundary conditions for the perfect electric conductor and perfect magnetic conductor are given by following equations

$$\mathbf{n} \times \mathbf{E} = 0, \quad \mathbf{n} \cdot \mathbf{B} = 0 \quad (PEC) \tag{1a}$$

$$\mathbf{n} \times \mathbf{H} = 0, \quad \mathbf{n} \cdot \mathbf{D} = 0 \quad (PMC) \tag{1b}$$

where $\mathbf{n}$ denotes the unit vector normal to the boundary surface. The PEMC boundary conditions are of more general form

$$\mathbf{n} \times (\mathbf{H} + M\mathbf{E}) = 0, \quad \mathbf{n} \cdot (\mathbf{D} - M\mathbf{B}) = 0 \quad (PEMC) \tag{2}$$

the latter condition can also be written as

$$\mathbf{n} \cdot (\epsilon_0 \mathbf{E} - M\mu_0 \mathbf{H}) = 0 \tag{3}$$

put together, these can be expressed as the vector condition

$$\mathbf{ME} = -\mathbf{H} + (\mathbf{1} + \mathbf{M^2}\eta_\mathbf{0}^\mathbf{2})\mathbf{nn} \cdot \mathbf{H}, \quad \eta_\mathbf{0} = \sqrt{\mu_\mathbf{0}/\epsilon_\mathbf{0}} \tag{4}$$

where M denotes the admittance of the PEMC boundary. PMC corresponds to $M = 0$ while PEC is obtained as the limit $M \to \pm\infty$. These conditions have a basic theoretical intrust because, in differential form formalism [3, 4], they correspond to the simplest possible medium by a single scalar medium parameter M [1]. The medium is also called the axon. Because PEMC does not allow electromagnetic energy to enter, it can serve as boundary material. The most notable difference is the nonreciprocity of the PEMC boundary when M has a finite nonzero value. Nonreciprocity of the PEMC boundary can be demonstrated by showing that the polarization of plane wave reflected from its surface is rotated, the sense and angle of rotation depending on the admittance parameter M. The PEMC medium can be represented as the limit of a bi-isotropic medium with infinite values for all of its four parameters $\epsilon = qM$, $\mu = \frac{q}{M}$, $\xi = \zeta = q$, $q \to \infty$. Focusing systems [5–8] and PEMC medium [9–23] have been discussed by many authors.

Here, we have extended our previous work [24] to a new Gregorian system, in which main reflector is PEMC while sub-reflector is PEC, by evaluating the field which is valid in the caustic region of a PEMC cylindrical Gregorian system by using Maslove's method. Maslov's method is a systematic procedure for predicting field in the caustic region. Maslov's method has been reviewed and applied by many authors [25–44].

2. RECEIVING CHARACTERISTIC OF CYLINDRICAL GREGORIAN REFLECTOR

Gregorian system consists of two reflectors, one is parabolic main reflector (PEMC in present discussion) and another is elliptical sub reflector (PEC). Gregorian system has many advantages over a single parabolic reflector. The system provides an attractive option for controlling the amplitude and the phase in the quiet zone. The single parabolic reflector does not allow much control over the aperture power distribution except for what is achievable by changing the focal length of the single parabolic reflector. The Gregorian reflector has an extra degree of freedom to control the aperture field distribution. In general, Gregorian reflector have shorter main reflector focal lengths,

and hence are more compact than conventional parabolic reflectors, but suffers performance degradation due to substantial interference from the secondary reflector. Additional benefits of Gregorian system include the ability to place the feed at a convenient location, and to reduce spillover and side-lobe radiation.

The equation of each reflector is given by

$$\zeta_1 = \frac{\xi_1^2}{4f} - f + c \tag{5}$$

$$\zeta_2 = a\left[\frac{1-{\xi_2}^2}{b^2}\right]^{\frac{1}{2}} \tag{6}$$

where

$$c^2 = a^2 - b^2, \quad aR_2 = c\zeta_2 - a^2, \quad aR_1 = c\zeta_2 + a^2$$

where (ξ_1, ζ_1) and (ξ_2, ζ_2) are the Cartesian coordinates of the point on the parabolic and elliptical reflectors, respectively.

Incident wave is given by

$$\mathbf{E^i} = \mathbf{u_y}\exp(jkz)$$

Thus the geometrical ray expression of the reflected wave is

$$\mathbf{E}^r = \mathbf{E}_0^r J^{\frac{-1}{2}} \exp[-jk(S_0 + t_1 + t + \phi_1)] \tag{7}$$

where

$$\begin{aligned}
J(t) &= \frac{D(t)}{D(0)} = \frac{1}{D(0)}\frac{\partial(x,z)}{\xi_1, t} \\
&= \frac{1}{D(0)}\begin{vmatrix} \dfrac{\partial\xi_2}{\partial\xi_1} + \dfrac{\partial p_{x2}}{\partial\xi_1}t & \dfrac{\partial\zeta_2}{\partial\xi_1} + \dfrac{\partial p_{z2}}{\partial\xi_1}t \\ p_{x2} & p_{z2} \end{vmatrix} \\
&= \frac{1}{D(0)}\left[-2\frac{\partial(\psi-\alpha)}{\partial\xi_1}t - \frac{\cos(\psi-2\alpha)}{\cos\psi}\frac{\partial\xi_2}{\partial\xi_1}\right] \\
&= 1 - \frac{t}{R_1} \\
R_1 &= \sqrt{(c+\zeta_2)^2 + \xi_2^2} \\
S_0 &= -\zeta_1 = 2f\frac{\cos 2\alpha}{1+\cos 2\alpha} - c \\
t_1 &= \sqrt{(\xi_2-\xi_1)^2 + (\zeta_2-\zeta_1)^2}, \\
t &= \sqrt{(x-\xi_2)^2 + (z-\zeta_2)^2} \\
\xi_1 &= 2f\tan\alpha
\end{aligned}$$

$$\begin{aligned}
\zeta_1 &= \frac{\xi_1^2}{4f} - f + c \\
\xi_2 &= \frac{b^2 \sin\psi}{\sqrt{c^2\cos\psi - b^2}} \\
\zeta_2 &= \frac{a^2 \sin\psi}{\sqrt{c^2\cos\psi - b^2}} \\
\tan\psi &= \frac{a\sin 2\alpha}{c + a\cos 2\alpha}
\end{aligned} \tag{8}$$

The initial value $\mathbf{E_0^r}(a)$ is obtained by

$$\mathbf{E_0^r} = \tilde{R} \cdot \mathbf{E_i}$$

The reflection dyadic is defined by

$$\begin{aligned}
\tilde{R} &= R_{co}\tilde{I} + R_{cr}\tilde{J} \\
\tilde{I} &= u_x u_x + u_y u_y \\
\tilde{J} &= u_z \times \tilde{I}
\end{aligned}$$

where *co* means co-polarized while cr means cross polarized. substitute $\mathbf{E}$ and $\mathbf{H}$ in boundary condition (4)

$$\mathbf{E}_0^r = -\frac{1}{\cos^2\alpha + M^2\eta_0^2}\left[(M^2\eta_0^2 - \cos^2\alpha)\mathbf{E_i} - 2M\eta_0\cos\alpha(\mathbf{u_z}\times\mathbf{E_i})\right] \tag{9}$$

$$\tilde{R} = -\frac{1}{\cos^2\alpha + M^2\eta_0^2}\left[(M^2\eta_0^2 - \cos^2\alpha)\tilde{I} - 2M\eta_0\cos\alpha\tilde{J}\right] \tag{10}$$

$$R_{co} = -\frac{M^2\eta_0^2 - \cos^2\alpha}{\cos^2\alpha + M^2\eta_0^2} \tag{11a}$$

$$R_{cr} = \frac{2M\eta_0\cos\alpha}{\cos^2\alpha + M^2\eta_0^2} \tag{11b}$$

The rotation angle is obtained as

$$\tan\phi_1 = \frac{R_{cr}}{R_{co}} = -\frac{2M\eta_0\cos\alpha}{M^2\eta_0^2 - \cos^2\alpha} \tag{12}$$

It is readily seen that the GO expression of the reflected wave becomes infinity at the point F_2 as is expected. We can derive the expression which is valid at the focal point using Maslov's method by

using the following expression by [35]

$$\mathbf{E}^r = \sqrt{\frac{k}{j2\pi}} \int_{-\infty}^{\infty} \mathbf{E}_0^r \left[\frac{D(t)}{D(0)} \frac{\partial p_{z2}}{\partial z}\right]^{\frac{-1}{2}} \exp -jk[S_0 + t_1 + t - z(x, p_{z2})p_z + zp_{z2} + \phi_1]dp_{z2} \quad (13)$$

The value of $\left[J(t)\frac{\partial p_{z2}}{\partial z}\right]^{\frac{-1}{2}}$ is given by by [35]

$$\left[J(t)\frac{\partial p_{z2}}{\partial z}\right]^{\frac{-1}{2}} = \frac{\sqrt{R_1}}{\sin(2\psi - 2\alpha)}$$

The phase function $S(p_z)$ is given by [35]

$$S(p_z) = S_0 + t_1 + S_{ex} + \phi_1$$

where

$$S_{ex} = -\rho\cos(2\psi - 2\alpha + \phi) + \xi_2 \sin(2\psi - 2\alpha) + \zeta_2 \cos(2\psi - 2\alpha)$$

$$\tan\phi = \frac{x}{z}$$

Field expression may be written as

$$\mathbf{E^r}(x, z) = \sqrt{\frac{k}{j2\pi}} \left[\int_{A1}^{A2} + \int_{-A2}^{-A1}\right] (R_{co}\mathbf{u}_y - R_{cr}\mathbf{u}_x)\sqrt{R_1} \exp[-jk(S_0 + t_1 + S_{ex} + \phi_1)]d(2\alpha) \quad (14)$$

When $M = \pm\infty$ (PEC), $R_{cr} = 0$, $R_{co} = -1$, therefore (13) becomes as

$$E^r(x, z) = \sqrt{\frac{k}{j2\pi}} \left[\int_{A_1}^{A_2} + \int_{-A_2}^{-A_1}\right] \sqrt{R_1} \exp[-jk(S_0 + t_1 + S_{ex})]d(2\alpha) \quad (15)$$

In the above equation R_1, S_0, t_1 and S_{ex} are expressed in terms of α and A_1, A_2 are the subtention angles 2α at the edges of the parabolic and hyperbolic cylinders.

3. RESULT AND DISCUSSION

Field pattern around the caustic of a two dimensional PEMC Gregorian reflector antenna are determined using Equation (13) by performing the integration numerically. Figure 2 and Figure 3 contain the

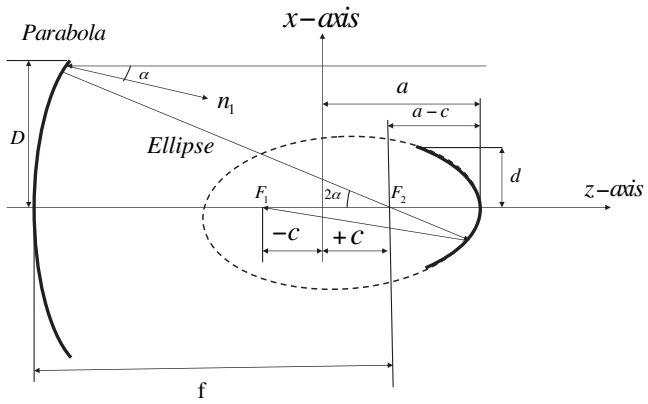

Figure 1. Gregorian system.

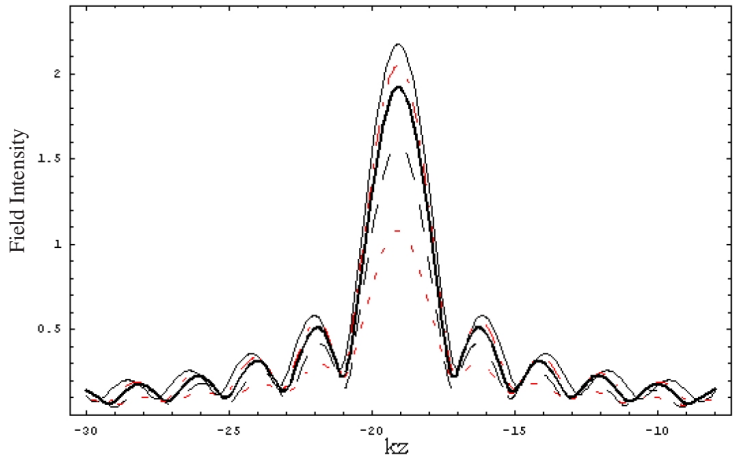

Figure 2. Comparison of *co* polarized field distribution along z-axis for $M\eta_0 = 600000$ (solid line), $M\eta_0 = 5.1$ (dot dashed line), and $M\eta_0 = 3.5$ (thick solid line), $M\eta_0 = 2.2$ (long dashed line), and $M\eta_0 = 0.5$ (dashed line).

comparison of plots of co-polarized field distribution for different value of $M\eta_0$ along z-axis and x-axis respectively. Plot for $M\eta_0 = 600000$ is in good agreement with two dimensional PEC Gregorian reflector antenna, that is, field patterns of Equation (14). Figure 4 and Figure 5 contain the comparison of plots of cross polarized field distribution different values of $M\eta_0$. For $M\eta_0 = 600,000$ field vanishes. Figure 6 to Figure 9 contain the comparison of plots of co-polarized field and

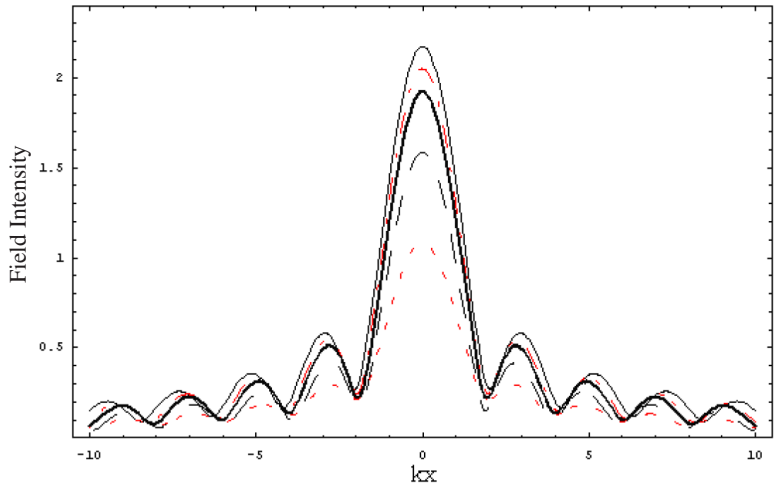

Figure 3. Comparison of *co* polarized field distribution along x-axis for $M\eta_0 = 600000$ (solid line), $M\eta_0 = 5.1$ (dot dashed line), and $M\eta_0 = 3.5$ (thick solid line), $M\eta_0 = 2.2$ (long dashed line), and $M\eta_0 = 0.5$ (dashed line).

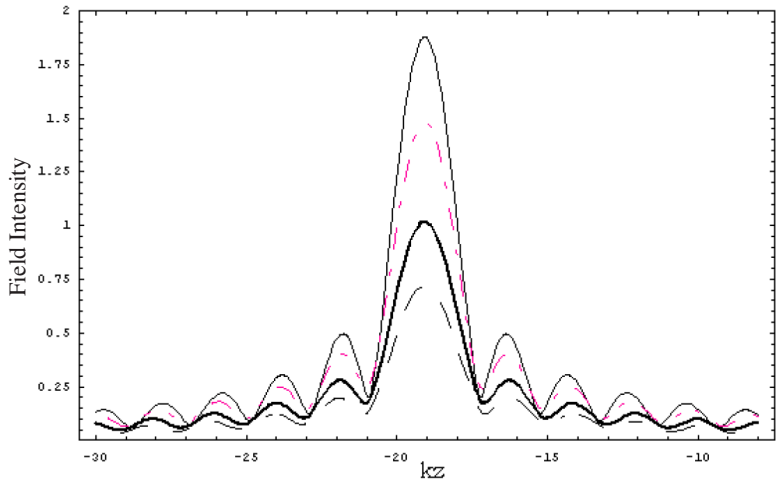

Figure 4. Comparison of cross polarized field distribution along z-axis for $M\eta_0 = 0.5$ (solid line), $M\eta_0 = 2.2$ (dot dashed line), and $M\eta_0 = 3.5$ (thick solid line), $M\eta_0 = 5.1$ (long dashed line), and $M\eta_0 = 600000$ (no plot).

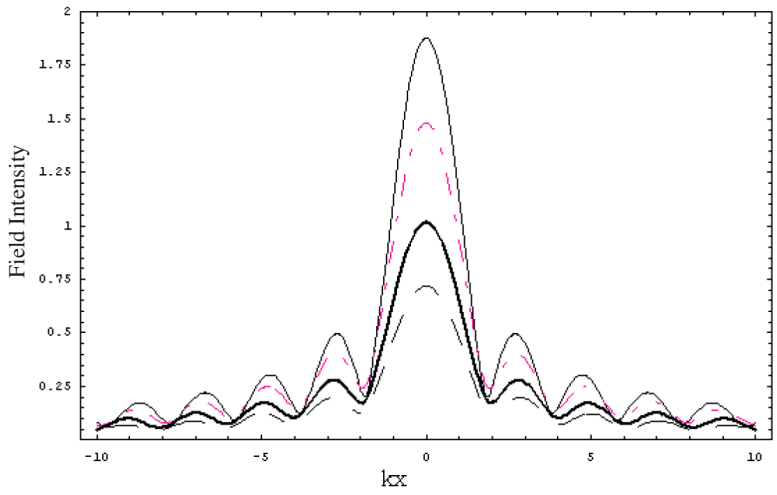

Figure 5. Comparison of cross polarized field distribution along x-axis for $M\eta_0 = 0.5$ (solid line), $M\eta_0 = 2.2$ (dot dashed line), and $M\eta_0 = 3.5$ (thick solid line), $M\eta_0 = 5.1$ (long dashed line), and $M\eta_0 = 600000$ (no plot).

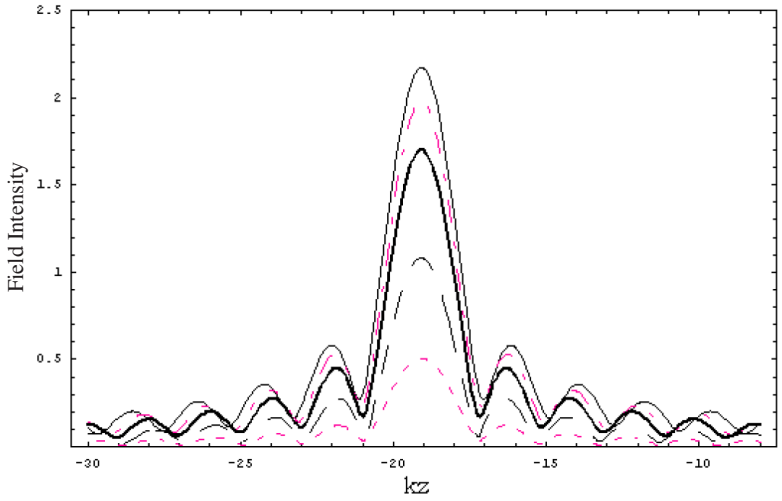

Figure 6. Comparison of *co* polarized field distribution along z-axis for $M\eta_0 = 500000$ (solid line), $M\eta_0 = 4.1$ (dot dashed line), and $M\eta_0 = 2.5$ (thick solid line), $M\eta_0 = 1.5$ (long dashed line), and $M\eta_0 = 1.1$ (dashed line).

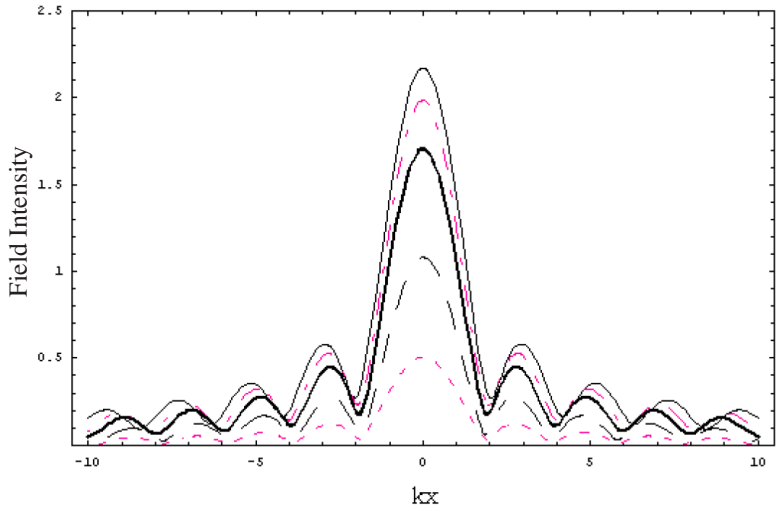

Figure 7. Comparison of *co* polarized field distribution along x-axis for $M\eta_0 = 500000$ (solid line), $M\eta_0 = 4.1$ (dot dashed line), and $M\eta_0 = 2.5$ (thick solid line), $M\eta_0 = 1.5$ (long dashed line), and $M\eta_0 = 1.1$ (dashed line).

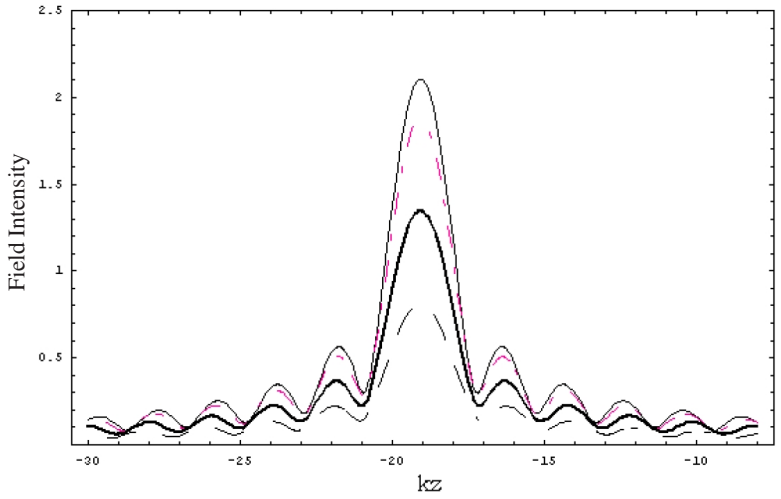

Figure 8. Comparison of cross polarized field distribution along z-axis for $M\eta_0 = 1.1$ (solid line), $M\eta_0 = 1.5$ (dot dashed line), and $M\eta_0 = 2.5$ (thick solid line), $M\eta_0 = 4.1$ (long dashed line), and $M\eta_0 = 500000$ (no plot).

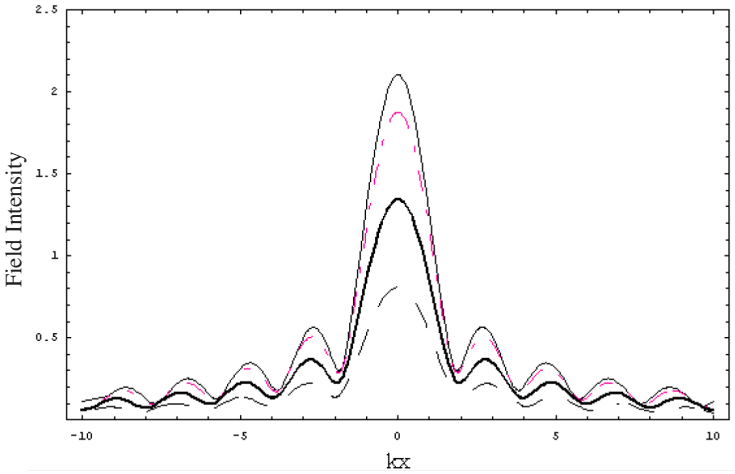

Figure 9. Comparison of cross polarized field distribution along x-axis for $M\eta_0 = 1.1$ (solid line), $M\eta_0 = 1.5$ (dot dashed line), and $M\eta_0 = 2.5$ (thick solid line), $M\eta_0 = 4.1$ (long dashed line), and $M\eta_0 = 500000$ (no plot).

cross polarized field distribution For all plots, it is assumed that at $kf = 25$, $a = 20$, $b = 6$, $d = 9$, $D = 20$. The location of the caustic may be observed and verified easily. It is observed from comparison that cross polarized field intensity decreases as $M\eta_0$ increases. Cross polarized field components vanish for $M\eta_0$ approaches to infinity and *co* polarized field intensity increases as $M\eta_0$ increases till it approaches to results of two dimensional PEC Gregorian reflector antenna the field patterns of Equation (14). It may be noted that limits of the integrals in Equation (13) are selected using the following relations by

$$A_1 = \phi_\nu = 2\arctan\left(\frac{D}{2f}\right)$$

$$A_2 = \arctan\left(\frac{d}{2c}\right)$$

REFERENCES

1. Lindell, I. V. and A. H. Sihvola, "Perfect electromagnetic conductor," *Journal of Electromagnetic Waves and Applications*, Vol. 19, No. 7, 861–869, 2005.
2. Lindell, I. V. and A. H. Sihvola, "Realization of the PEMC

boundary," *IEEE Trans. Antennas Propag.*, Vol. 53, 3012–3018, Sep. 2005.

3. Dechamps, G. A., "Electromagnetics and differential forms," *Proc. IEEE*, Vol. 69, 676–696, 1981.
4. Lindell, I. V., *Differential Forms in Electromagnetics*, Willey IEEE press, New York, 2004.
5. Gizesik, J. A., "Focusing properties of a three-parameter class of oblate, Luneberg-like inhomogeneous lenses," *Journal of Electromagnetic Waves and Applications*, Vol. 19, No. 8, 1005–1019, 2005.
6. Nikolic, N., J. S. Kot, and S. Vinogradov, "Scattering by a Luneberg Lens partially covered by a metallic cap," *Journal of Electromagnetic Waves and Applications*, Vol. 21, No. 4, 549–563, 2007.
7. Boutayeb, H., A.-C. Tarot, and K. Mahdjoubi, "Focusing characteristics of a metallic cylindrical electromagnetic band gap structure with defects," *Progress In Electromagnetics Research*, PIER 66, 89–103, 2006.
8. Vinogradov, S. S., P. D. Smith, J. S. Kot, and N. Nikolic, "Radar cross-section studies of spherical lens reflectors," *Progress In Electromagnetics Research*, PIER 72, 325–337, 2007.
9. Lindell, I. V. and A. H. Sihvola, "Transformation method for problems involving perfect electromagnetic conductor (PEMC) structures," *IEEE Trans. on Antennas and Propagation*, Vol. 53, No. 9, 3005–3011, Sep. 2005.
10. Lindell, I. V. and A. H. Sihvola, "Losses in PEMC boundary," *IEEE Trans. on Antennas and Propagation*, Vol. 54, No. 9, 2553–2558, Sept. 2006.
11. Lindell, I. V. and A. H. Sihvola, "The PEMC resonator," *Journal of Electromagnetic Waves and Applications*, Vol. 20, No. 7, 849–859, 2006.
12. Hehl, F. W. and Y. N. Obukhov, "Linear media in classical electrodynamics and post constraint," *Phys. Lett. A*, Vol. 334, 249–259, 2005.
13. Obukhov, Y. N. and F. W. Hehl, "Measuring a piecewise constant axon field in classical electrodynamics," *Phys. Lett. A*, Vol. 341, 357–365, 2005.
14. Jancewicz, B., "Plane electromagnetic wave in PEMC," *Journal of Electromagnetic Waves and Applications*, Vol. 20, No. 5, 647–659, 2006.
15. Ruppin, R., "Scattering of electromagnetic radiation by a perfect

electromagnetic conductor sphere," *Journal of Electromagnetic Waves and Applications*, Vol. 20, No. 12, 1569–1576, 2006.

16. Ruppin, R., "Scattering of electromagnetic radiation by a perfect electromagnetic conductor cylinder," *Journal of Electromagnetic Waves and Applications*, Vol. 20, No. 13, 1853–1860, 2006.
17. Lindell, I. V., A. H. Sihvola, S. A. Tretyakov, and A. J. Viitanen, *Electromagnetic Waves in Chiral and Bi-Isotropic Media*, Artech House, Norwood, MA, 1994.
18. Hansen, R. C., *Geometrical Theory of Diffraction*, IEEE Press, New York, NY, 1988.
19. Felson, L. B., *Hybrid Formulation of Wave Propagation and Scattering*, Nato ASI Series, Martinus Nijhoff, Dordrecht, The Netherlands, 1984.
20. Hussain, A. and Q. A. Naqvi, "Perfect electromagnetic conductor (PEMC) and fractional waveguide," *Progress In Electromagnetics Research*, PIER 73, 61–69, 2007.
21. Hussain, A., Q. A. Naqvi, and M. Abbas, "Fractional duality and perfect electromagnetic conductor," *Progress In Electromagnetics Research*, PIER 71, 85–94, 2007.
22. Ahmed, S. and Q. A. Naqvi, "Electromagnetic scattering from a perfect electromagnetic conductor cylinder buried in a dielectric half-space," *Progress In Electromagnetics Research*, PIER 78, 25–38, 2008.
23. Ahmed, S. and Q. A. Naqvi, "Electromagnetic scattering from a parallel perfect electromagnetic conductor cylinders of circular cross-sections using an iterative procedure," *Journal of Electromagnetic Waves and Applications*, Vol. 22, 987–1003, 2008.
24. Fiaz, M. A., A. Ghaffar, and Q. A. Naqvi, "High frequency expressions for the field in the caustic region of a PEMC cylindrical reflector using Maslov's method," *Journal of Electromagnetic Waves and Applications*, Vol. 22, 358–397, 2008.
25. Kravtsov, Y. A., "Two new methods in the theory of wave propagation in inhomogeneous media (review)," *Sov. Phys. Acoust.*, Vol. 14, No. 1, 1–17, 1968.
26. Gorman, A. D., S. P. Anderson, and R. B. Mohindra, "On caustic related to several common indices of refraction," *Radio Sci.*, Vol. 21, 434–436,1986.
27. Gorman, A. D., "Vector field near caustics," *J. Math. Phys.*, Vol. 26, 1404–1407, 1985.
28. Hongo, K., Y. Ji, and E. Nakajimi, "High-frequency expression for the field in the caustic region of a reflector using Maslov's

method," *Radio Sci.*, Vol. 21, No. 6, 911–919, 1986.

29. Hongo, K. and Y. Ji, "High-frequency expression for the field in the caustic region of a cylindrical reflector using Maslov's method," *Radio Sci.*, Vol. 22, No. 3, 357–366, 1987.
30. Hongo, K. and Y. Ji, "Study of the field around the focal region of spherical reflector antenna by Maslov's method," *IEEE Trans. Antennas Propagat.*, Vol. 36, 592–598, May 1988.
31. Ji, Y. and K. Hongo, "Field in the focal region of a dielectric spherical by Maslov's method," *J.Opt. Soc. Am. A*, Vol. 8, 1721–1728, 1991.
32. Ji, Y. and K. Hongo, "Analysis of electromagnetic waves refracted by a spherical dielectric interface by Maslov's method," *J.Opt. Soc. Am. A*, Vol. 8, 541–548, 1991.
33. Hongo, K. and H. Kobayashi, "Radiation characteristics of a plano convex lens antenna," *Radio Sci.*, Vol. 31, No. 5, 1025–1035, 1987.
34. Aziz, A., Q. A. Naqvi, and K. Hongo, "Analysis of the fields in two dimensional Cassegrain system," *Progress In Electromagnetics Research*, PIER 71, 227–241, 2007.
35. Aziz, A., A. Ghaffar, Q. A. Naqvi, and K. Hongo, "Analysis of the fields in two dimensional Gregorian system," *Journal of Electromagnetic Waves and Applications*, Vol. 22, No. 1, 85–97, 2008.
36. Ghaffar, A., Q. A. Naqvi, and K. Hongo, "Analysis of the fields in three dimensional Cassegrain system," *Progress In Electromagnetics Research*, PIER 72, 215–240, 2007.
37. Ghaffar, A., A. Hussain, Q. A. Naqvi, and K. Hongo, "Radiation characteristics of an inhomogeneous slab," *Journal of Electromagnetic Waves and Applications*, Vol. 22, No. 2, 301–312, 2008.
38. Ghaffar, A., Q. A. Naqvi, and K. Hongo, "Study of focusing of field refracted by a cylindrical plano-convex lens into a uniaxial crystal by using Maslov's method," *Journal of Electromagnetic Waves and Applications*, Vol. 22, 665–679, 2008.
39. Hussain, A., Q. A. Naqvi, and K. Hongo, "Radiation characteristics of the Wood lens using Maslov's method," *Progress In Electromagnetics Research*, PIER 73, 107–129, 2007.
40. Faryad, M. and Q. A. Naqvi, "High frequency expressions for the field in the caustic region of a cylindrical reflector placed in chiral medium," *Progress In Electromagnetics Research*, PIER 76, 153–182, 2007.

41. Faryad, M. and Q. A. Naqvi, "Cylindrical reflector in chiral medium supporting simultaneously positive phase velocity and negative phase velocity," *Journal of Electromagnetic Waves and Applications*, Vol. 22, 563–572, 2008.
42. Ghaffar, A., Q. A. Naqvi, and K. Hongo, "Focal region fields of three dimensional Gregorian system," *Optics Communications*, 2007.
43. Ashraf, M. R., A. Ghaffar, and Q. A. Naqvi, "Fields in the focal space of symmetrical hyperbolic focusing lens using Maslov's method," *Journal of Electromagnetic Waves and Applications*, Vol. 22, 815–828, 2008.
44. Faryad, M. and Q. A. Naqvi, "High frequency field in the caustic region of a parabolic reflector coated with isotropic chiral medium," *Journal of Electromagnetic Waves and Applications*, Vol. 22, 965–986, 2008.